# DETECTION OF PNEUMONIA USING CONVOLUTIONAL NEURAL NETWORK AND DEEP LEARNING

**A PROJECT REPORT**

Submitted in partial fulfillment of the requirements for the award of the internship

**By**

Pamu Chandu (21331A05D7)

Varisi Anuhya (21331A05I1)

Grandhi Sai Hemanth Kumar (21331A0557)

(Students of MAHARAJ VIJAYARAM GAJAPATHI RAJ COLLEGE OF ENGINEERING (A))

**Supervisor:**

**Dr. Mohammad Farukh Hashmi**

**Assistant Professor**

**Department of Electronics and Communication Engineering**


**Department of Electronics and Communication Engineering**

**National Institute of Technology, Warangal**

**2023-24**

## ABSTRACT:

To investigate the prospects, uses, and technology of the detection of pneumonia using convolutional neural networks and deep learning, this study provides a thorough review.This work uses a synthetic approach to select relevant research sources. This In addition to offering an updated model for detecting pneumonia, which will be used in our upcoming research, the paper surveys and compares the detection of lung disease using several computer-aided techniques. In the study, the most popular datasets, including Google Scholar, were searched. Approximately thirty publications were collected, of which fifteen underwent in-depth examination based on the topic of interest. Additionally, the review paper emphasizes the significance of COVID-19, pneumonia, tuberculosis, and normal. Humans can contract pneumonia, a potentially fatal bacterial disease that primarily affects one or both lungs and is brought on by the bacteria Streptococcus pneumoniae. Convolutional neural networks (CNNs) have received a lot of interest for illness categorization as a result of the effectiveness of deep learning algorithms for the analysis of medical pictures. Furthermore, pre-trained CNN models' characteristics from massive datasets come in useful for picture classification jobs. The statistical findings show how useful pretrained CNN models combined with supervised classifier algorithms can be in the analysis of chest X-ray pictures, particularly in the diagnosis of pneumonia.

**Keywords**: Chest X-ray pictures, pneumonia, deep learning, transfer learning, convolution neural network (CNN), and computer-aided diagnosis.

## 1. INTRODUCTION:

Indoor air pollution is one of the main causes of pneumonia in children. Pneumonia is a severe acute respiratory illness that affects many people in age groups at extreme of the average human lifespan. It is caused by infectious organisms with high attack rates [1].In the US alone, pneumonia causes over a million adult hospital admissions and almost 50,000 deaths each year [2].Doctors diagnose pneumonia in hospital patients in a number of ways, including physical examination, medical history, clinical investigations (such as sputum or blood tests), chest X-rays, and several other imaging techniques. William Osler referred to pneumonia as "the captain of the men of death" in the 1800s.

Computer-aided designs (CAD) have emerged as the key area of machine learning research in recent years. CAD can lessen workload pressure, increase inter- and intra-reader variability, and enhance diagnostic accuracy [3]. Inspired by the brain's visual cortex, convolutional neural networks (CNNs) are utilized to handle challenging image-driven pattern recognition problems by identifying both linear and nonlinear patterns [4].Convolutional Neural Networks (CNNs), in particular, have demonstrated their self-potential to extract valuable features in image classification tasks when used as Deep Learning (DL) models[5,6].

VGG16, VGG19, ResNet50 and its variations, Inception-v3 and its variations, MobileNetV3, DenseNet121, and EfficientNetb0 are transfer learning models that are available on Keras. Pneumonia patients have symptoms in the chest cavity such as fluids filling the lungs' air sacs,

and their radiological picture appears brighter. The goal of the work is to create CNN models from keras that have high validation accuracy, recall, and F1 score, and can identify pneumonic patients from chest X-rays. The effectiveness of deep learning approaches has been demonstrated, and their accuracy in predicting diseases is comparable to that of an average radiology [7]. Numerous tests are available for diagnosing pneumonia, including computed tomography of the lungs, needle biopsy of the lung, chest MRI, chest X-ray, and chest ultrasound.

The contributions are as follows.

1) A CNN model is trained using images to identify several diseases, including Tuberculosis, Pneumonia, Covid19, and Normal.

2)Modifications to the model cause variations in their mutual accuracy. To increase the model's accuracy, the CNN model's layers are altered.

3)Model accuracy, loss, and model evaluation metrics like f1 score, recall, and precision increase with the choice of optimizer (Adamax), adjustments to pre-processing, data augmentation, and fine-tuning parameters like rotation, flip, learning rate, epochs, and batch size.

## 2. LITERATURE SURVEY:

The challenge of classifying chest x-ray pictures into different classes has been considerably explored in the realm of medical diagnosis. Researchers have attempted to apply several methods for decreasing dimensionality in [8]. The artificial neural network was tested by the authors in [9] to detect lung disorders, such as tuberculosis, pneumonia, and lung cancer. Recently, there has been an increase in interest in the field of medical picture classification for the investigation of machine learning (ML) algorithms for the detection of thoracic disorders. A technique for identifying pulmonary tuberculosis was presented by Lakhani and Sundaram (2017) [10], based on the architecture of two distinct CNNs, AlexNet and Google Net. To detect pneumonia at a level that is superior to that of radiologists, Pranav Rajpurkar, Jeremy Irvin, et al. (2017) [11] recently investigated this dataset. They called their model Chex Net, and it employs DenseNet-121layer architecture to detect all 14 diseases from the large number of 112,200 images that are available in the dataset.

Researchers use chest X-ray scans to present a strategy for identifying lung cancer in [12].A modified CNN that was carefully regulated was utilized in the study [13] to diagnose X-ray thorax illness in the chest. A CNN model was introduced by Anthimopoulos et al. [14] to detect patterns of interstitial lung disease.14,696 images represent the seven classes in the dataset that was used to train it. 85.5% accuracy was achieved by their model.Krizhevsky et al. [15] demonstrated that deep CNN models can produce innovative outcomes on challenging datasets, with a top 5 error percentage of 17%. The ImageNet dataset was the one selected. There are sixty million people in their network overall. Parameters and features max-pooling layers in addition to five convolutional layers. For best outcomes, three fully connected layers were

employed. Following the development of the Chex Net [24] model, Benjamin Antin et al. (2017) [16] examined the dataset [11] and suggested a logistic regression model for the identification of pneumonia.

Numerous fields have previously adopted deep learning-based techniques [17–21]. Numerous biomedical image detection methods have already been proposed by various authors'. Razaak [22] talked about the difficulties and prospects for medical image processing. CNNs operate on the basis of the features that are retrieved by the different layers in order to correctly recognize and categorize the different types of chest X-rays. Using a deep CNN and a 2.5D resampling technique, Roth et al. [23] developed an algorithm for lymph node detection in computed tomography data. To prevent any errors in diagnosis, the chest X-ray images are put through an evaluation procedure called scan line optimization, which filters out any other body areas. A visualization strategy for localizing the region of interest in the chest X-rays was reported by Rajaraman et al. [24]. CNN model was used by Rahib et al. [25] and Okeke et al. [26] to classify pneumonia cases.

In this paper, we took datasets with 3 classes and a TB dataset, then we made another dataset with 4 classes by combining these two. We applied the CNN model to get better accuracy.

## 3. METHODS:

### 3.1. CNN:

A class of deep neural networks called convolutional neural networks (CNN) is used to analyse visual imagery. It is made up of numerous hidden layers, an input layer, and an output layer [27]. A CNN-based machine learning system was used to classify the images. One type of deep learning neural network is the CNN [28]. In our CNN model, we employed ten layers in total: two dense layers, a flatten layer, a dropout layer, three MaxPooling2D layers, and three Convolution2D layers.

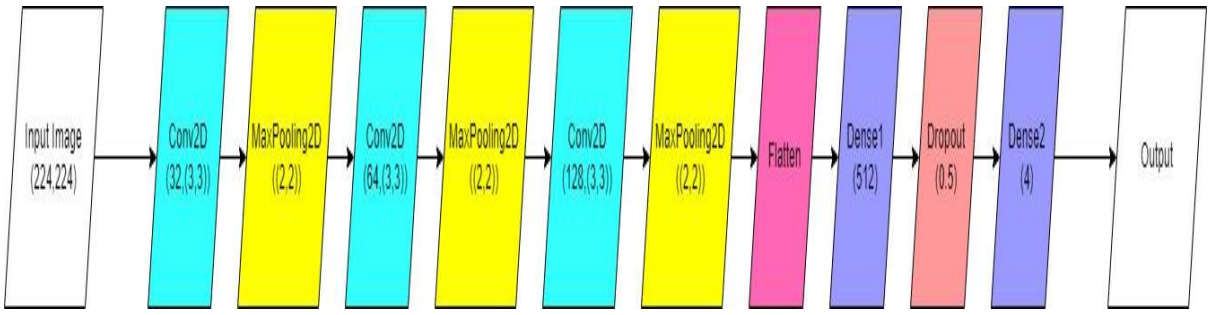


**Fig-1: CNN** Sample Architecture

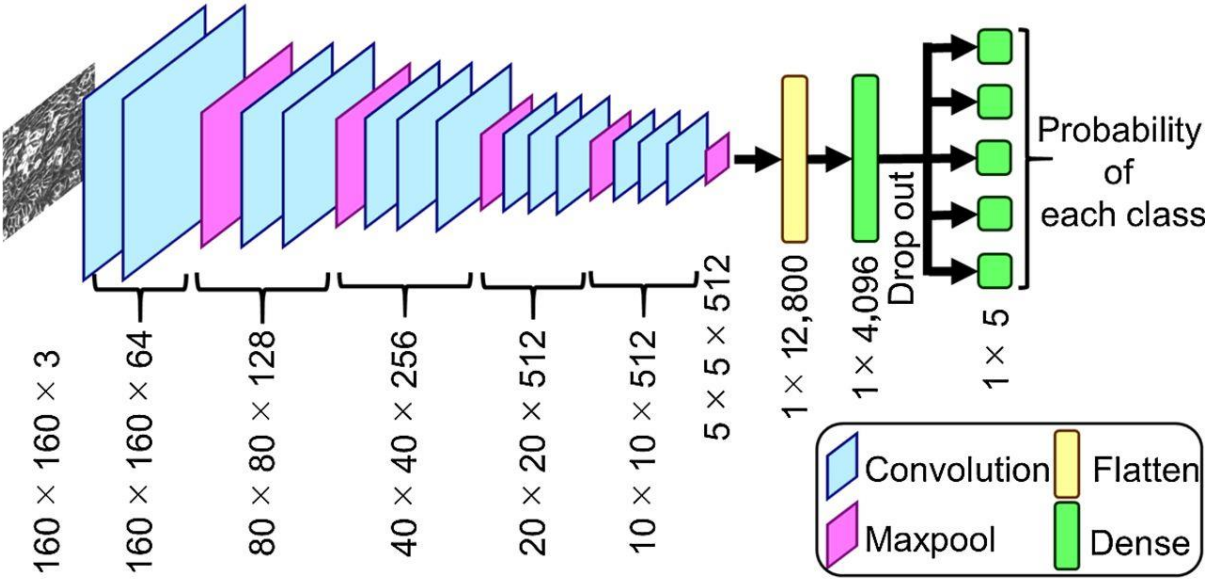


**Fig-2: CNN** Model Architecture

### 3.1.1. ConvolutionLayer:

A picture input is transformed into a matrix form. A feature map is produced when the input matrix and a feature detector, filter, or kernel of dimension 3X3 are subjected to the convolution operation [29]. The image's size is decreased during this operation, simplifying image processing. This also results in information loss, but the feature detector keeps the essential components of the picture [30].

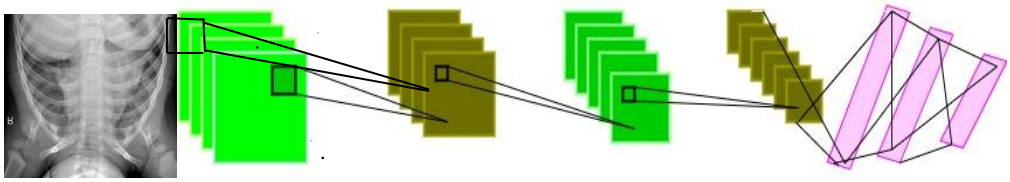

**Chest Xray Convolution Layer Pooling Layer Convolution LayerPooling layer SoftMax Final output**

**Fig-3:** Convolutional neural network consisting of convolution and pooling layers and fullyconnected SoftMax layers at the end to give the final prediction

### 3.1.2. Max-Pooling Layer:

The pooling layer's objective is to further down sample the input image. To put it another way, to make the input image smaller [31]. As a result of the image's fewer parameters, the computational complexity is decreased. The models employ the max-pooling and average-pooling subsampling techniques. A sample-based discretization technique is called max-pooling. Each feature map is processed by the dimension 2X2 pooling layer, which uses the 'MAX' function to scale the dimensionality. The highest pixel value from the image window that the feature detector is currently covering is chosen using max pooling [32]. Pooling layer is a feature extraction operation, which is typically applied in Convolutional Neural Network(CNN).

### 3.2. TRANSFER LEARNING:

Transfer learning is a powerful deep learning technique. Applying a model that has already been trained to a new problem is known as transfer learning. Transfer learning is a technique whereby pre-trained machine learning model data is migrated to a different but related model. Transfer learning is a concept that may be used to a smaller dataset by using a trained model from a larger dataset, such as ImageNet, as shown in Figure 2 [33]. In machine learning (ML), transfer learning is used. In Transfer Learning, a machine makes better generalization about one job by using the knowledge it has learned from an earlier one.

In this case, X is a specific learning sample (X = x1, · · ·, xn, ∈ χ), xi is the ith term vector corresponding to certain texts, and χ is the space of all term vectors.
The task T for a given domain D is defined with the following parameters:
T = {γ, P (Y | X)} = {γ, Y = {y1, · · ·, yn}, yi ∈ γ (1)

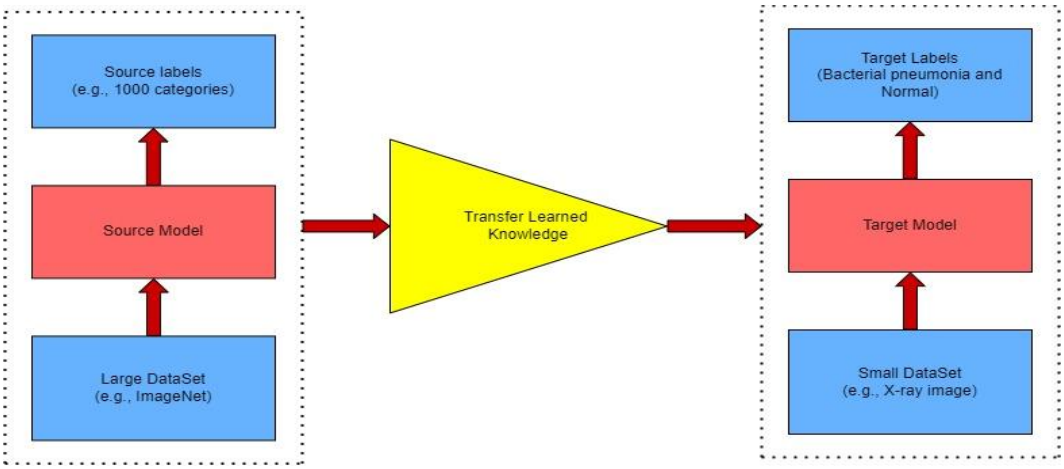


**Fig-4:** Concept of Transfer learning

## 4. MATERIALS:

### 4.1. EXPERIMENTAL DATASET:

The combination of the Covid19 chest x-ray, tuberculosis, and pneumonia datasets is the dataset that we used. The datasets we downloaded from Kaggle include Chest X-ray Images (Pneumonia) [34], Chest X-ray (Covid-19 & Pneumonia), Curated COVID-19 Chest X-Ray Dataset, and Tuberculosis (TB) Chest X-ray Cleaned Database.
The base folders are named Test, Train, and Valid, while the subfolders of each folder are named Covid19, Normal, Pneumonia, and Tuberculosis. Chest x-ray images are classified(Categorical data) and placed separately in Covid19, Normal, Pneumonia, Tuberculosis sub folders of Test, Train, Valid.

| Category | Training Set | Validation Set | Testing Set |
|---|---|---|---|
| **Normal** | 2650 | 654 | 234 |
| **Pneumonia** | 8917 | 861 | 411 |
| **Covid19** | 1025 | 256 | 116 |
| **Tuberculosis** | 2650 | 150 | 700 |
| **Total** | 15242 | 1921 | 1461 |
| **Percentage** | 82 | 10 | 8 |

**Table 1.** Description of the experimental dataset.

18624 chest x-ray pictures from the Covid19, Normal, Pneumonia, and Tuberculosis classes are included in our collection. The Train Dataset contains 15242 photos, the Valid Dataset has 1921 images, and the Test dataset contains 1461 images.

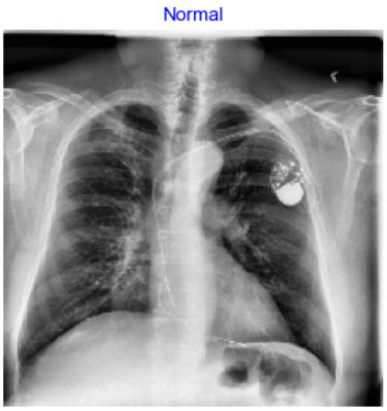


a) Chest x-ray of healthy person

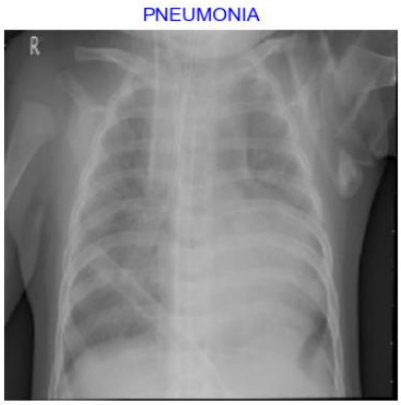


b) Person suffering with pneumonia

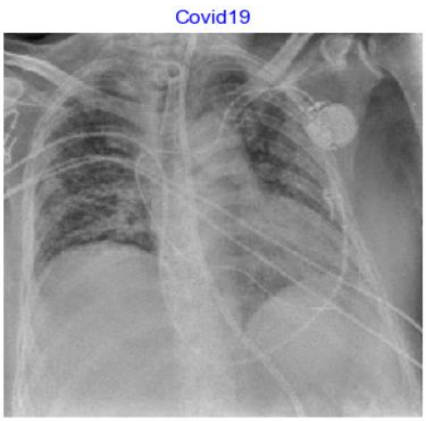


c) Person suffering with Covid-19

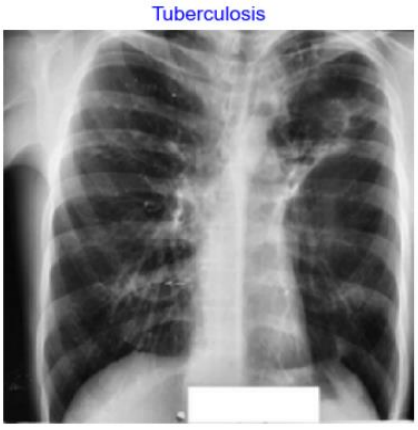


d) Person suffering with T.B

**Fig-5:** Sample images

## 5. PROPOSED METHODOLOGY:

This research proposes an optimal approach for the identification of pneumonia from chest X-rays. Techniques for data augmentation were used to expand the little dataset. The final prediction was then calculated by combining the predictions from these models with a weighted classifier. Figure 5 displays the whole block diagram of the suggested technique.

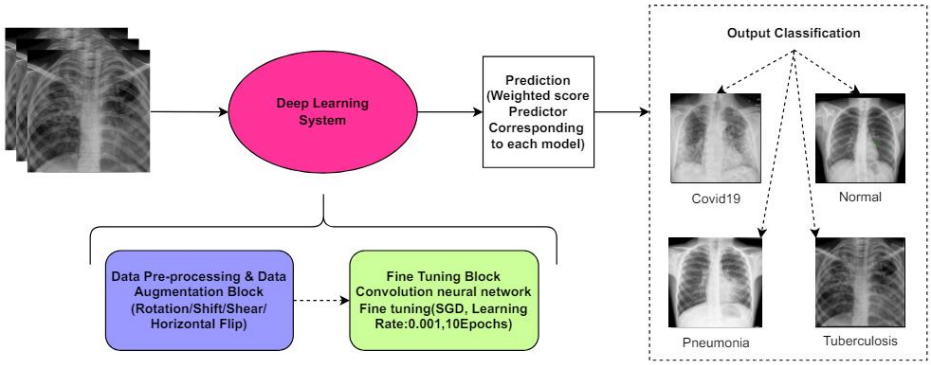


**Fig-6:** Block diagram of the proposed methodology

### 5.1. PRE-PROCESSING & DATA AUGMENTATION:

Resizing the X-ray images was a crucial step in the data preprocessing process because different algorithms required varied image input sizes [35]. We set the model's input size to 224,224,3, where 224,224 is the image form and 3 is the number of channels (R, G, and B). Thus, we changed the form of our input image to 224,224.

| | filepaths | label |
|---|---|---|
| 0 | E:\Sai\C19_P_TB\Dataset\Dataset_1\Train\Covid1... | Covid19 |
| 1 | E:\Sai\C19_P_TB\Dataset\Dataset_1\Train\Covid1... | Covid19 |
| 2 | E:\Sai\C19_P_TB\Dataset\Dataset_1\Train\Covid1... | Covid19 |
| 3 | E:\Sai\C19_P_TB\Dataset\Dataset_1\Train\Covid1... | Covid19 |
| 4 | E:\Sai\C19_P_TB\Dataset\Dataset_1\Train\Covid1... | Covid19 |
| ... | ... | ... |
| 15237 | E:\Sai\C19_P_TB\Dataset\Dataset_1\Train\Tuberc... | Tuberculosis |
| 15238 | E:\Sai\C19_P_TB\Dataset\Dataset_1\Train\Tuberc... | Tuberculosis |
| 15239 | E:\Sai\C19_P_TB\Dataset\Dataset_1\Train\Tuberc... | Tuberculosis |
| 15240 | E:\Sai\C19_P_TB\Dataset\Dataset_1\Train\Tuberc... | Tuberculosis |
| 15241 | E:\Sai\C19_P_TB\Dataset\Dataset_1\Train\Tuberc... | Tuberculosis |

15242 rows × 2 columns

**Fig-7:** Pre-processing Train Dataset

| | filepaths | label |
|---|---|---|
| 0 | E:\Sai\C19_P_TB\Dataset\Dataset_1\Valid\Covid1... | Covid19 |
| 1 | E:\Sai\C19_P_TB\Dataset\Dataset_1\Valid\Covid1... | Covid19 |
| 2 | E:\Sai\C19_P_TB\Dataset\Dataset_1\Valid\Covid1... | Covid19 |
| 3 | E:\Sai\C19_P_TB\Dataset\Dataset_1\Valid\Covid1... | Covid19 |
| 4 | E:\Sai\C19_P_TB\Dataset\Dataset_1\Valid\Covid1... | Covid19 |
| ... | ... | ... |
| 1916 | E:\Sai\C19_P_TB\Dataset\Dataset_1\Valid\Tuberc... | Tuberculosis |
| 1917 | E:\Sai\C19_P_TB\Dataset\Dataset_1\Valid\Tuberc... | Tuberculosis |
| 1918 | E:\Sai\C19_P_TB\Dataset\Dataset_1\Valid\Tuberc... | Tuberculosis |
| 1919 | E:\Sai\C19_P_TB\Dataset\Dataset_1\Valid\Tuberc... | Tuberculosis |
| 1920 | E:\Sai\C19_P_TB\Dataset\Dataset_1\Valid\Tuberc... | Tuberculosis |

1921 rows × 2 columns

**Fig-8:** Pre-processing Valid Dataset

| | filepaths | label |
|---|---|---|
| 0 | E:\Sai\C19_P_TB\Dataset\Dataset_1\Test\COVID19... | COVID19 |
| 1 | E:\Sai\C19_P_TB\Dataset\Dataset_1\Test\COVID19... | COVID19 |
| 2 | E:\Sai\C19_P_TB\Dataset\Dataset_1\Test\COVID19... | COVID19 |
| 3 | E:\Sai\C19_P_TB\Dataset\Dataset_1\Test\COVID19... | COVID19 |
| 4 | E:\Sai\C19_P_TB\Dataset\Dataset_1\Test\COVID19... | COVID19 |
| ... | ... | ... |
| 1456 | E:\Sai\C19_P_TB\Dataset\Dataset_1\Test\Tubercu... | Tuberculosis |
| 1457 | E:\Sai\C19_P_TB\Dataset\Dataset_1\Test\Tubercu... | Tuberculosis |
| 1458 | E:\Sai\C19_P_TB\Dataset\Dataset_1\Test\Tubercu... | Tuberculosis |
| 1459 | E:\Sai\C19_P_TB\Dataset\Dataset_1\Test\Tubercu... | Tuberculosis |
| 1460 | E:\Sai\C19_P_TB\Dataset\Dataset_1\Test\Tubercu... | Tuberculosis |

1461 rows × 2 columns

**Fig-9:** Pre-processing Test Dataset

Data augmentation makes better use of already-existing data to address this issue. It helps make the current training dataset larger and prevents the model from overfitting this dataset.

Below are images following various enhancement approaches (Figure 9). For the creation of the augmented image, just one of these methods was applied.

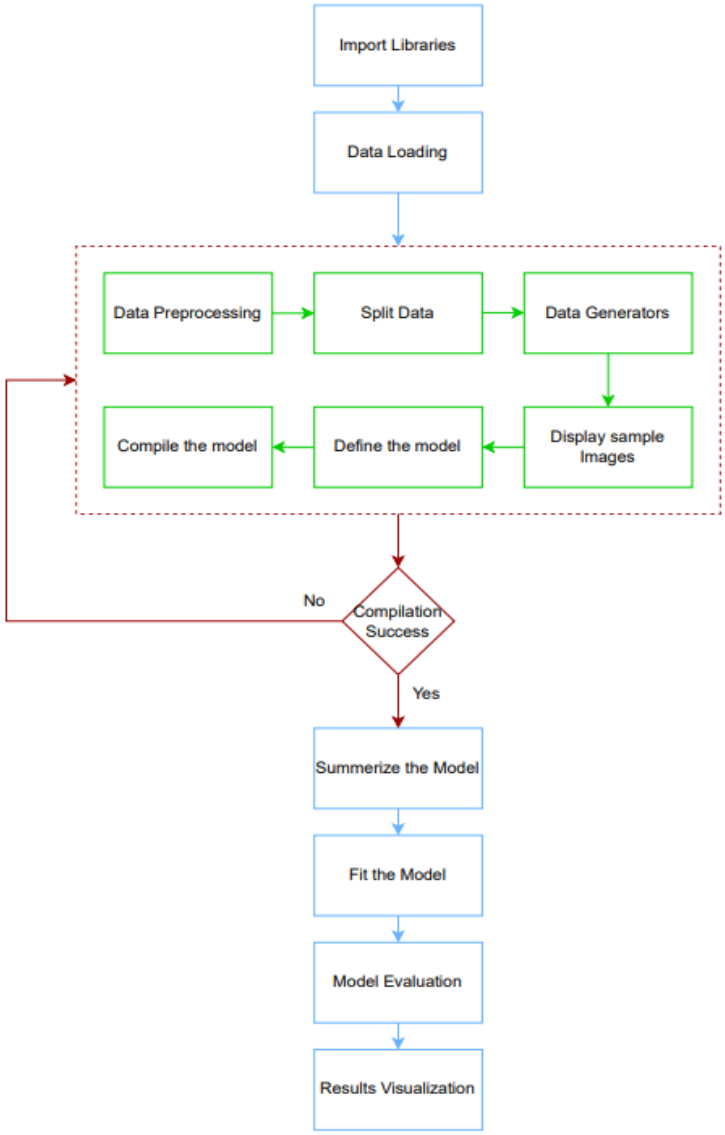


**Fig-10:** Flow chart of CNN model

## 6. EXPERIMENTAL SETUP :

This section presents the experiments and assessment methods utilized in the research to assess the suggested model's efficacy. Utilized was the chest X-ray image collection that was suggested in. The pre-trained architectures were loaded onto the ImageNet Dataset using the open-source Keras deep learning framework, which was then tuned for the given job using

TensorFlow as the backend. A standard PC equipped with an Intel i7 seventh-generation CPU, 8 GB RAM, and an NVIDIA GeForce GTX 1060 6 GB GPU handled all of the processing work.

| Parameters | Values |
|---|---|
| Number of Classes | 4 |
| Image Size | (224,224) |
| Channels | 3 |
| Batch Size | 256 |
| Epochs | 20 |
| Optimizer | Adamax |
| Learning Rate | 0.001 |
| Activation Function | Sigmoid, relu |
| Loss Function | categorical_crossentropy |

**Table-2:**Experimental setup of CNN model

## 7. EXPERIMENT RESULTS AND DISCUSSION:

A collection of 16 images from the training dataset are shown, along with the names of their classes. It initially pulls data from the training generator, including class names and related indices. It then obtains a collection of pictures together with their captions. It displays each of the first 16 photographs in this batch in a 4x4 grid and normalizes the pixel values for better viewing. Each image's title is set to the name of its class, which is found in the label array by identifying the class with the highest probability. For a more polished appearance, the axes are off. The plot is finally shown.

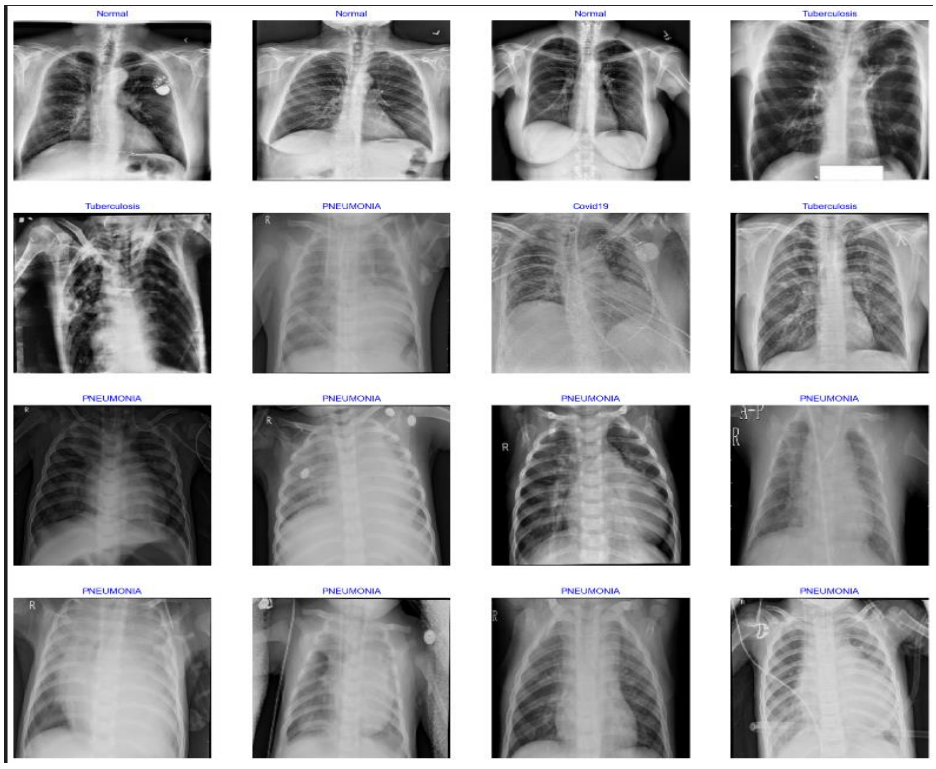


**Fig-11:** Images of different diseases

## RESULTS:

We also worked on existing models to get more knowledge and to understand models clearly. After implementing those models we got these results.

| Architecture | Accuracy | Precision | Recall | F1 Score |
|---|---|---|---|---|
| ResNet50 | 97.29 | 97.03 | 98.25 | 97.62 |
| DenseNet121 | 98.00 | 96.53 | 99.00 | 98.26 |
| MobilNetV2 | 96.71 | 96.08 | 98.25 | 97.15 |
| EfficientNetB0 | 98.86 | 99.00 | 100.00 | 99.00 |
| CNN | 97.70 | 98.00 | 98.00 | 97.00 |

**Table-3:** Accuracy, precision, recall, F1 score corresponding to different architectures

ResNet50 efficiently identifies true positives and performs well with high recall. There may be a few extra false positives because its precision is little lower than its recall.
Out of all the architectures, DenseNet121 has the highest recall, meaning it detects nearly all true positives. But compared to ResNet50, its precision is smaller, indicating more false positives.
Among the architectures, MobileNetV2 has the lowest accuracy but the highest recall. Its largest false positive rate is shown by its lowest precision.
The maximum accuracy, perfect recall, and utmost precision are achieved by EfficientNetB0, outperforming all other architectures. This shows that it performs the best, having extremely few false positives and no false negatives.
The overall CNN performs well overall, with great recall and precision. While it is more accurate than MobileNetV2, it is marginally less accurate than EfficientNetb0.

### 7.1. Result in Terms of Testing Accuracy and Testing Loss:

The proposed work is implemented in python language using Jupyter notebook. First, we trained this dataset using CNN model. But we did not get better result. Later, we modified some layers in order to get better results and also increased epochs up to 20. We concerned about loss function, optimizer, epochs, batch size, and layers which reflects better results.

Each experiment was carried out five times in order to test and assess the suggested network's performance. Throughout the training, parameters and hyperparameters were adjusted. The training accuracy and training loss curves acquired after 10 epochs of model training are displayed. Every model has a training accuracy greater than 99% and a training loss of less than 0.03. All of the other models, with the exception of exception, had training loss curves and accuracy that were comparable.

| | Accuracy | Loss |
|---|---|---|
| **Training** | 99.9% | 0.001 |
| **Validation** | 97.7% | 0.093 |
| **Testing** | 98.2% | 0.071 |

**Table-4:**Model Evaluation

The machine learning model's performance metrics during its three phases of training, validation, and testing are shown in the table.
99.9% of the training data are correctly classified by the model during the training phase.A loss of 0.001, which is incredibly low, shows how well the model has absorbed the training set.

The validation stage's accuracy of 97.7% shows how well the model performs on the validation set, which is used to fine-tune the model. Although 97.7% accuracy is high, it is less than the training accuracy, suggesting a minor decline in performance and we got loss of 0.093 which means it performed well.
The model's performance on the test set is represented by its accuracy of 98.2% in the testing state, which is used to evaluate the final model. Furthermore impressive is the accuracy of 98.2%, which shows how effectively the model generalizes to fresh, untested data.An excellent sign of generalization is the test set loss of 0.071, which is larger than the training loss but lower than the validation loss.

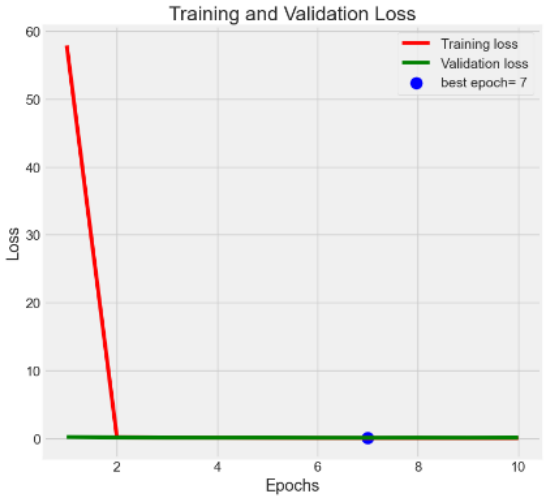


**Fig-12:**Training and validation loss

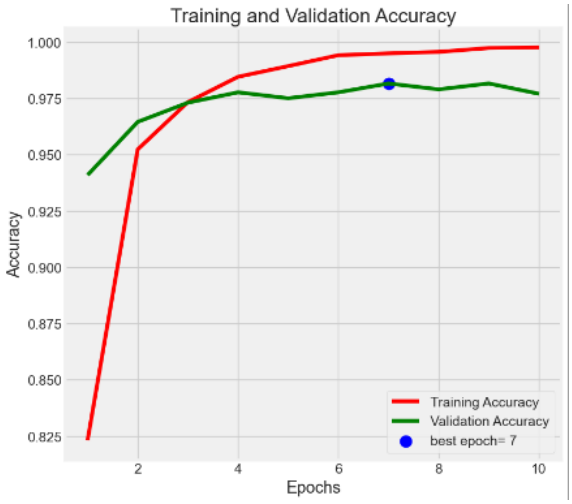


**Fig-13:**Training and validation accuracy

The above graphs show the accuracy and loss during training and validation for a machine learning model over a number of epochs.

Within the first epoch, the training loss rapidly drops from a relatively high starting point to almost zero.This sharp decline suggests that the model picks up the training set fast, resulting in little loss during the initial stages of training.
Throughout the training process, the validation loss is relatively flat and begins at a low value.This flat line indicates that while training goes on, the model's performance on the validation set remains mostly unchanged.
Epoch 7 is chosen as the best epoch, signifying the moment at which, in terms of a selected metric (likely validation loss or accuracy), the validation performance is at its best.

## 7.2. Performance Analysis:

We applied the CNN model and got the following confusion matrix. Following the conclusion of the training phase, each model was evaluated using the test dataset. F1, area under the curve,

accuracy, recall, precision was used to validate their performance. The discussion of each performance statistic utilized in this article follows.

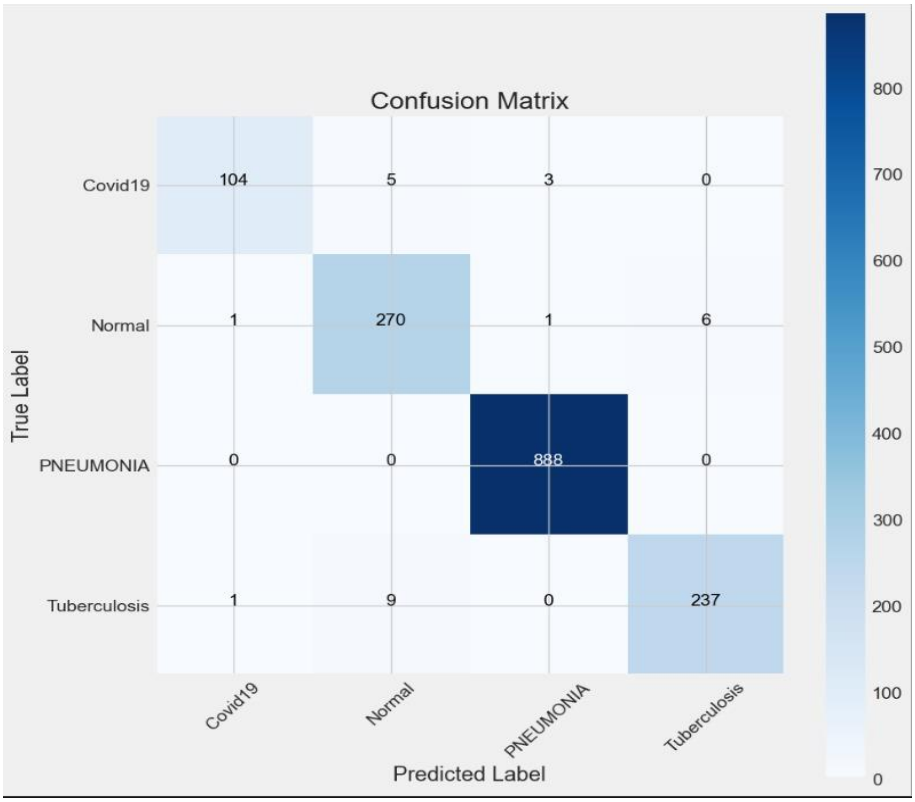


**Fig-14:** Test data (CNN model)

True positive (TP) indicates the number of pneumonia images identified as pneumonia, true negative (TN) indicates the number of normal images identified as normal (healthy), false positive (FP) indicates the number of normal images incorrectly identified as pneumonia images, and false negative (FN) indicates the number of pneumonia images incorrectly identified as normal. These definitions and equations are used to classify patients into healthy and pneumonia patients.

- Accuracy: It indicates the degree to which the measured value resembles a known value.
  Accuracy = (TP + FN)/ (TP + TF + FP + FN) **(2)**
- Precision: This indicates the model's level of accuracy with respect to positively anticipated data.

  Precision = TP / (TP + FP) **(3)**

- Recall: After classifying something as positive, it determines how many real positives the model caught (true positives).

  Recall = TP / (TP + FN) **(4)**

- F1: It provides a recall and accurate balancing.

  F1 = 2 × (Recall × Precision) / (Recall + Precision) **(5)**

| | precision | recall | f1-score | Support |
|---|---|---|---|---|
| **Covid19** | 0.98 | 0.93 | 0.95 | 112 |
| **Normal** | 0.95 | 0.97 | 0.96 | 278 |
| **Pneumonia** | 1.00 | 1.00 | 1.00 | 888 |
| **Tuberculosis** | 0.98 | 0.96 | 0.97 | 247 |

**Table-5:**Classification Report

According to classification report we can observe that:

1) With 112 cases, "Covid19" has a f1-score of 0.95, recall of 0.93, and precision of 0.98.

2) With 278 instances, "normal" has a f1-score of 0.96, recall of 0.97, and precision of 0.95.
3) With 888 instances, "pneumonia" has a f1-score of 1.00, precision and recall of 1.00.
4) With 247 instances, "tuberculosis" has a f1-score of 0.97, recall of 0.96, and precision of 0.98.
The model performs well in every category, according to this classification report.

### 7.3. ROC CURVE:

The suggested classifier and the ROC curves for various designs are displayed in Figure 15.

The suggested classifier was able to obtain the highest AUC score of 97.7%. Every model displayed a comparable AUC/ROC curve. The weighted classifier produced the greatest results, according to the analysis, with an AUC score of 97.7%, an F1 score of 1.00, and a test accuracy of 98%.

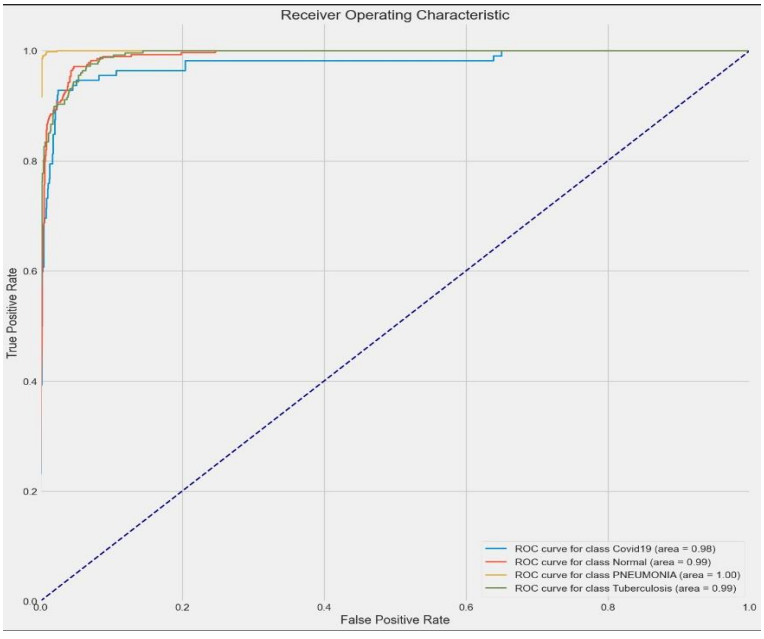


**Fig-15:** ROC Curve

| | precision | recall | f1-score | Support |
|---|---|---|---|---|
| **Covid19** | 0.98 | 0.93 | 0.95 | 112 |
| **Normal** | 0.95 | 0.97 | 0.96 | 278 |
| **Pneumonia** | 1.00 | 1.00 | 1.00 | 888 |
| **Tuberculosis** | 0.98 | 0.96 | 0.97 | 247 |

**Table 6**: Accuracy, precision, recall, F1 score, and AUC score corresponding to architectures.

Classification performance metrics for several classes in a multi-class classification problem are shown in the above table.The classes are Covid19, Normal, Pneumonia, and Tuberculosis.

- Covid19: Excellent recall and precision, but marginally worse recall than other classes, which results in a marginally lower F1-score.
- Normal: Good performance with a slightly higher recall than precision, showing high precision and recall.
- Pneumonia: Pneumonia occurrences are flawlessly classified by the model, as seen by perfect scores for all criteria.
- Tuberculosis: Good performance is indicated by a balanced and high F1-score, together with excellent precision and recall.

### 7.4. COMPARATIVE ANALYSIS OF VARIOUS EXISTING METHODS:

The accuracy of the suggested methodology was compared to other current methods. The authors have published all of the findings in this section in their individual research.

| Model | No. of Images | Precision | Recall | Accuracy | AUC |
|---|---|---|---|---|---|
| P Bertin et al. [37] | 5232 | 90.1 | 93.2 | 92.8 | 99 |
| S Candemir et al. [38] | 5856 | 97.0 | 99.5 | 96.2 | 99 |
| B Ergen et al. [39] | 5849 | 96.88 | 96.83 | 96.84 | 96.8 |
| DBS Santos et al. [40] | 5840 | 94.3 | 94.5 | 94.4 | 94.5 |
| Halil Murat Unver et al. [41] | 5856 | 91.3 | 89.1 | 84.5 | 87 |
| Saad Kashem et al. [42] | 5247 | 97 | 99 | 98 | 98 |
| Sanjay Kumar Singh et al. [43] | 5232 | 93.28 | **99.6** | 96.39 | **99.34** |
| Proposed Methodology | 78624 | **98** | 98 | **99** | 99 |

**Table 7:** Comparison of the proposed methodology with different existing methods.

A DenseNet-121-based model was employed by P Bertin et al. [37]. They stated that their AUC was 98.4%. Regretfully, the paper did not report the other measures. S Candemir et al. [38] reported a test accuracy of 96.2% using customised CNNs to identify pneumonia. B. Ergen et al. [39] classified pneumonia with 96.84% accuracy by combining features from several deep learning models. Sanjay Kumar Singh et al. [43] used majority voting to aggregate the outputs of several neural networks to arrive at the final forecast. They received a 99.34 AUC score. Using deep learning-based techniques, DBS Santos et al. [40], Halil Murat Unver et al. [41], and Saad Kashem et al. [42] obtained accuracy of 94.4%, 84.5%, and 98.0%, respectively. The size of the datasets used in each of these studies was comparable. Table 7 summarizes all of the results that were previously addressed.

## 8. CONCLUSION AND FUTURE SCOPE:

In this paper, we attempt to find a simpler approach for pneumonia detection for chest X-ray images by comparing the different architectures on the same dataset. Based on our findings, we selected the most perfect model, which is easy to train and has one of the best performance metrics. There are several approaches to detecting pneumonia using CNN, and it gives better accuracy, recall, and F1 score. We are using deep learning algorithms that have proven to be more realistic. It can also be observed that the accuracy of the network can be increased by preprocessing techniques. CNN model to provide efficient accuracy and best solution for the pneumonia detection based on the chest X-ray images.

For the first, we got less validation accuracy and less training accuracy, so we trained this model again and again. After training the CNN model, we got a validation accuracy of 97% and a training accuracy of 99%.

We also show that the simple extension of our algorithm that can perform on multiple diseases outperforms the previous state of the art on Chest X-ray images. The issue of not enough training for the dataset has also been addressed using data augmentation and transfer learning. In the future, an algorithm that can determine the areas of the lung damaged by pneumonia will be developed. The models of these convolutional neural networks were successfully created using a variety of parameter tuning techniques, including adding dropout, adjusting learning rates, modifying batch sizes, epoch counts, adding more complex fully connected layers, and adjusting different stochastic gradient optimizers [36].

## REFERENCES:


[1] Marrie, T. (1994). Community-acquired pneumonia. Clinical Infectious Diseases. 18(4), 501-513.

[2] CDC, 2017. URL https://www.cdc.gov/features/ pneumonia/index.html.

[3] Sayed E., et. al, “Computer-aided Diagnosis of Human Brain Tumor though MRI: A Survey and a new algorithm. Expert System with Applications (41) : 2014.

[4] C. Ciresan, U. Meier, J. Masci, L.M. Gambardella, J. Schmidhuber, Highperformance neural networks for visual object classification, (2011), arXiv preprint arXiv:1102.0183.

[5] Ali Sharif Razavian, Hossein Azizpour, Josephine Sullivan, and Stefan Carlsson. 2014. CNN features off-the-shelf: an astounding baseline for recognition. In Proceedings of the IEEE conference on computer vision and pattern recognition workshops. 806813.

[6] Nijhawan, Rahul, Rose Verma, Shashank Bhushan, Rajat Dua, and Ankush Mittal. ”An Integrated Deep Learning Framework Approach for Nail Disease Identification.” In Signal-Image Technology and InternetBased Systems (SITIS), 20

[7] Hosny A, Parmar C, Quackenbush J, et al. Artificial intelligence in radiology. Nat Rev Cancer. 2018;18(8): 500–510. doi:10.1038/s41568-018-0016-5

[8] Gang, Peng, Wang Zhen, Wei Zeng, Yuri Gordienko, Yuriy Kochura, Oleg Alienin, Oleksandr Rokovyi, and Sergii Stirenko. "Dimensionality reduction in deep learning for chest x-ray analysis of lung cancer." In 2018 Tenth International Conference on Advanced Computational Intelligence (ICACI), pp. 878-883. IEEE, 2018.

[9] Khobragade, Shubhangi, Aditya Tiwari, C. Y. Patil, and Vikram Narke. "Automatic detection of major lung diseases using Chest Radiographs and classification by feed-forward artificial neural network." In 2016 IEEE 1st International Conference on Power Electronics, Intelligent Control and Energy Systems (ICPEICES), pp. 1-5. IEEE, 2016.

[10] Paras Lakhani and Baskaran Sundaram. 2017. Deep learning at chest radiography: automated classification of pulmonary tuberculosis by using convolutional neural networks. Radiology 284, 2 (2017), 574582.

[11] Pranav Rajpurkar, Jeremy Irvin, Kaylie Zhu, Brandon Yang, Hershel Mehta, Tony Duan, Daisy Ding, Aarti Bagul, Curtis Langlotz, Katie Shpanskaya, and others. 2017. Chexnet: Radiologist-level pneumonia detection on chest x-rays with deep learning. arXiv preprint arXiv:1711.05225 (2017).

[12] Udeshani, K. A. G., R. G. N. Meegama, and T. G. I. Fernando. "Statistical feature-based neural network approach for the detection of lung cancer in chest x-ray images." International Journal of Image Processing (IJIP) 5, no. 4 (2011): 425-434.

[13] Guan, Qingji, Yaping Huang, Zhun Zhong, Zhedong Zheng, Liang Zheng, and Yi Yang. "Diagnose like a radiologist: Attention guided convolutional neural network for thorax disease classification." arXiv preprint arXiv:1801.09927 (2018).

[14] M. Anthimopoulos, S. Christodoulidis, L. Ebner, A. Christe, S. Mougiakakou, Lung pattern classification for interstitial lung diseases using a deep convolutional neural network, IEEE Trans. Med. Imaging 35 (5) (2016) 1207–1216.

[15] A. Krizhevsky, I. Sutskever, G.E. Hinton, Imagenet classification with deep convolutional neural networks, in: Advances in neural information processing systems, (2012), pp. 1097–1105.

[16] Benjamin Antin, Joshua Kravitz, and Emil Martayan. 2017. Detecting Pneumonia in Chest X-Rays with Supervised Learning. (2017).

[17] Douarre, C.; Schielein, R.; Frindel, C.; Gerth, S.; Rousseau, D. Transfer learning from synthetic data applied to soil–root segmentation in x-ray tomography images. J. Imaging 2018, 4, 65. [CrossRef]

[18] Zhang, Y.; Wang, G.; Li, M.; Han, S. Automated classification analysis of geological structures based on images data and deep learning model. Appl. Sci. 2018, 8, 2493. [CrossRef]

[19]Wang, Y.; Wang, C.; Zhang, H. Ship classification in high-resolution SAR images using deep learning of small datasets. Sensors 2018, 18, 2929. [CrossRef] [PubMed]

[20]Sun, C.; Yang, Y.; Wen, C.; Xie, K.; Wen, F. Voiceprint identification for limited dataset using the deep migration hybrid model based on transfer learning. Sensors 2018, 18, 2399. [CrossRef] [PubMed]

[21] Chen, Z.; Zhang, Y.; Ouyang, C.; Zhang, F.; Ma, J. Automated landslides detection for mountain cities using multi-temporal remote sensing imagery. Sensors 2018, 18, 821. [CrossRef]

[22] Razzak, M.I.; Naz, S.; Zaib, A. Deep learning for medical image processing: Overview, challenges and the future. In Classification in BioApps; Springer: Cham, Switzerland, 2018; pp. 323–350.

[23] Roth HR, et al. A new 2.5 D representation for lymph node detection using random sets of deep convolutional neural network observations. International conference on medical image computing and computer-assisted intervention; Springer, Cham; 2014.

[24] Rajaraman S, Candemir S, Kim I, et al. Visualization and interpretation of convolutional neural network predictions in detecting pneumonia in pediatric chest radiographs. Appl Sci. 2018;8(10):1715.

[25] Abiyev, R.H.; Ma'aitah, M.K.S. Deep convolutional neural networks for chest diseases detection. J. Healthc. Eng. 2018, 2018, 4168538. [CrossRef] [PubMed]

[26]Stephen, O.; Sain, M.; Maduh, U.J.; Jeong, D.U. An efficient deep learning approach to pneumonia classification in healthcare. J. Healthc. Eng. 2019, 2019, 4180949. [CrossRef] [PubMed]

[27]Shah, S., Mehta, H. and Sonawane, P., 2020, August. Pneumonia detection using convolutional neural networks. In *2020 Third International Conference on Smart Systems and Inventive Technology (ICSSIT)* (pp. 933-939). IEEE.

[28] Račić, L., Popović, T. and Šandi, S., 2021, February. Pneumonia detection using deep learning based on convolutional neural network. In *2021 25th International Conference on Information Technology (IT)* (pp. 1-4). IEEE.

[29] Xu, Y., Jia, Z., Ai, Y., Zhang, F., Lai, M., Eric, I. and Chang, C., 2015, April. Deep convolutional activation features for large scale brain tumor histopathology image classification and segmentation. In 2015 IEEE international conference on acoustics, speech and signal processing (ICASSP) (pp. 947-951). IEEE.

[30] Rubin, J., Sanghavi, D., Zhao, C., Lee, K., Qadir, A. and Xu-Wilson, M., 2018. Large scale automated reading of frontal and lateral chest x-rays using dual convolutional neural networks. *arXiv preprint arXiv:1804.07839*.

[31] Simonyan, K. and Zisserman, A., 2014. Very deep convolutional networks for large-scale image recognition. *arXiv preprint arXiv:1409.1556*.

[32]Xu, Y., Jia, Z., Ai, Y., Zhang, F., Lai, M., Eric, I. and Chang, C., 2015, April. Deep convolutional activation features for large scale brain tumor histopathology image classification and segmentation. In *2015 IEEE international conference on acoustics, speech and signal processing (ICASSP)* (pp. 947-951). IEEE.

[33] Wang, S.H., Xie, S., Chen, X., Guttery, D.S., Tang, C., Sun, J. and Zhang, Y.D., 2019. Alcoholism identification based on an AlexNet transfer learning model. *Frontiers in psychiatry*, *10*, p.454348.

[34] Kermany, Daniel; Zhang, Kang; Goldbaum, Michael (2018), "Labeled Optical Coherence Tomography (OCT) and Chest X-Ray Images for Classification", Mendeley Data, V2, doi: 10.17632/rscbjbr9sj.2

[35] Rahman, T., Chowdhury, M.E., Khandakar, A., Islam, K.R., Islam, K.F., Mahbub, Z.B., Kadir, M.A. and Kashem, S., 2020. Transfer learning with deep convolutional neural network (CNN) for pneumonia detection using chest X-ray. *Applied Sciences*, *10*(9), p.3233.

[36] Du, S. S., Zhai, X., Poczos, B., Singh, A.: Gradient Descent Provably Optimizes OverParameterized Neural Networks (2018). arXiv preprint arXiv:1810.02054

[37] Cohen, J.P.; Bertin, P.; Frappier, V. Chester: A Web Delivered Locally Computed Chest X-Ray Disease Prediction System. arXiv 2019, arXiv:1901.11210

[38] Rajaraman, S.; Candemir, S.; Kim, I.; Thoma, G.; Antani, S. Visualization and interpretation of convolutional neural network predictions in detecting pneumonia in pediatric chest radiographs. Appl. Sci. 2018, 8, 1715.

[39] To˘gaçar, M.; Ergen, B.; Cömert, Z. A deep feature learning model for pneumonia detection applying a combination of mRMR feature selection and machine learning models. IRBM 2019.

[40] Saraiva, A.; Santos, D.; Costa, N.J.C.; Sousa, J.V.M.; Ferreira, N.F.; Valente, A.; Soares, S. Models of Learning to Classify X-ray Images for the Detection of Pneumonia using Neural Networks. 2019.

[41] Ayan, E.; Ünver, H.M. Diagnosis of Pneumonia from Chest X-Ray Images Using Deep Learning. In Proceedings of the 2019 Scientific Meeting on Electrical-Electronics &

Biomedical Engineering and Computer Science (EBBT), Istanbul, Turkey, 2–26 April 2019; pp. 1–5.

[42] Rahman, T.; Chowdhury, M.E.; Khandakar, A.; Islam, K.R.; Islam, K.F.; Mahbub, Z.B.; Kadir, M.A.; Kashem, S. Transfer Learning with Deep Convolutional Neural Network (CNN) for Pneumonia Detection using Chest X-ray. Appl. Sci. 2020, 10, 3233

[43] Chouhan, V.; Singh, S.K.; Khamparia, A.; Gupta, D.; Tiwari, P.; Moreira, C.; Damaševi˘cius, R.; de Albuquerque, V.H.C. A Novel Transfer Learning Based Approach for Pneumonia Detection in Chest X-ray Images. Appl. Sci. 2020, 10, 559.